Effect of glucose substitution by low-molecular weight chitosan-derivatives on functional, structural and antioxidant properties of maillard reaction-crosslinked chitosan-based films

Sawsan Affes, Hana Maalej, Suming Li, Rania Abdelhedi, Rim Nasri, Moncef Nasri

HAL Id: hal-03930101

https://hal.umontpellier.fr/hal-03930101v1

Submitted on 11 Jan 2023

Food Chemistry

Effect of glucose substitution by low-molecular weight chitosan-derivatives on functional, structural and antioxidant properties of Maillard reaction-crosslinked chitosan-based films
--Manuscript Draft--

Corresponding Author:	hana maalej, Assistant Professor National School of Engineering of Sfax Sfax, TUNISIA
First Author:	Sawsan Affes, Doctor
Order of Authors:	Sawsan Affes, Doctor
	hana maalej, Assistant Professor
	Suming Li, Professor
	Rania Abdelhedi, Doctor
	Rim Nasri, Assistant professor
	Moncef Nasri, Professor
Abstract:	In this study, the effects of different temperatures, incubation times and types of reducing sugars, including glucose and different low molecular weight (Mw) chito-oligosaccharides (COS) with varying acetylation degree (AD), on the extent of Maillard reaction (MR) on chitosan-based films were studied. Interestingly, an improvement of structural and functional properties of all MR-crosslinked films was noted, which is more pronounced by heating at higher temperature and exposure time. These findings were proved through FTIR and X-ray diffraction analyses. In addition, color change and Ultraviolet spectra demonstrate that glucose addition provides the high extent of MR, followed by COS1 and COS2 . These results were confirmed by enhanced water resistance and thermal properties. Moreover, MR-chitosan/COS films showed the highest mechanical properties, whereas, glucose-loaded films were brittle, as demonstrated by scanning electron microscopy micrographs. Furthermore, MR-chitosan/COS1 films exhibited the better antioxidant behavior followed by chitosan/glucose and chitosan/COS2 films, mainly at higher heating-conditions.

Highlights

- Maillard reaction (MR) was induced in chitosan-glucose and chitosan/chito-oligosaccharides films;

- The type of reducing sugar involved in MR had a great impact on its extent;

- MR rate was influenced by temperature and heating time;

- Functional and structural properties of films were modified by heat treatments.

- Antioxidant properties were higly enhanced by the MR products.

Effect of glucose substitution by low-molecular weight chitosan-derivatives on functional, structural and antioxidant properties of Maillard reaction-crosslinked chitosan-based films

Sawsan Affes [1], Hana Maalej [1,2] [*], Suming Li [3], Rania Abdelhedi [4], Rim Nasri [1,5], Moncef Nasri [1]

[1] *Laboratory of Enzyme Engineering and Microbiology, National School of Engineering of Sfax (ENIS), University of Sfax, P.O. Box 1173, Sfax 3038, Tunisia.*

[2] *Department of Life Sciences, Faculty of Science of Gabes, Omar Ibn Khattab Street, Gabes 6029, Tunisia.*

[3] *Institut Européen des Membranes, IEM-UMR 5635, Univ Montpellier, ENSCM, CNRS, 34095 Montpellier, France.*

[4] *Laboratory of Molecular and Cellular Screening Processes, Centre of Biotechnology of Sfax, University of Sfax, Route Sidi Mansour, Po Box 1177, 3018 Sfax, Tunisia.*

[5] *Higher Institute of Biotechnology of Monastir, University of Monastir, Rue Taher Haddad, Monastir 5000, Tunisia.*

[*] Corresponding author: Hana Maalej

Address: B.P.68, 3021 Sfax, Tunisia

Tel: +216-20-234699; fax: +216-74-275-595.

E-mail address: hannou25@yahoo.fr

Abstract

In this study, the effects of different temperatures, incubation times and types of reducing sugars, including glucose and different low molecular weight (Mw) chito-oligosaccharides (COS) with varying acetylation degree (AD), on the extent of Maillard reaction (MR) on chitosan-based films were studied. Interestingly, an improvement of structural and functional properties of all MR-crosslinked films was noted, which is more pronounced by heating at higher temperature and exposure time. These findings were proved through Fourier-transform infrared and X-ray diffraction analyses. In addition, color change and Ultraviolet spectra demonstrate that glucose addition provides the high extent of MR, followed by COS1 (Mw < 4.4 kDa; AD, 18.20%) and COS2 (Mw < 4.4 kDa; AD, 10.63%). These results were confirmed by enhanced water resistance and thermal properties. Moreover, MR-chitosan/COS films showed the highest mechanical properties, whereas, glucose-loaded films were brittle, as demonstrated by scanning electron microscopy micrographs. Furthermore, MR-chitosan/COS1 films exhibited the better antioxidant behavior followed by chitosan/glucose and chitosan/COS2 films, mainly at higher heating-conditions. Thereby, MR-crosslinked chitosan/COS based films were attractive to be applied as functional and active coating-materials in various fields.

Keywords:

Chitosan; Chito-oligosaccharides; Films; Maillard reaction conditions; Physicochemical characterization; antioxidant potential.

1. Introduction

Nowadays, many research has been made to develop natural, biodegradable and non-toxic bio-based packaging to enhance the shelf-life of fresh or packaged commercialized food as alternative to synthetic packaging, which are the main cause of environmental pollution (Galiano et al., 2018; Liu et al., 2019). Indeed, coating material should protect food from all pathogenic contamination, oxidation and drying and perfectly prevent the Ultraviolet (UV) radiation. For this reason, several polymers such as polysaccharides and proteins were widely used for biofilm preparation (Affes et al., 2020; Etxabide, Urdanpilleta, Guerrero, & de la Caba, 2015; Gennadios, Handa, Froning, Weller & Hanna, 1998; Hamdi, Nasri, Ben Azaza, Li, & Nasri, 2020; Kchaou, Benbettaïeb, Jridi, Nasri, & Debeaufort, 2019). Thanks to its film-forming properties, antioxidant and antimicrobial activities, chitosan-based film has received growing interest to be applied in different fields including food, biotechnology, cosmetics and biomedical domains (Aranaz et al., 2018; Chang et al., 2019; Hajji, Younes, Affes, Boufi, & Nasri, 2018; Li, Lin, & Chen, 2014).

The physicochemical properties of chitosan films were depended on chitosan characteristics mainly its molecular weight (Mw), acetylation degree (AD) and depolymerization degree (Affes et al., 2021; Hamdi et al., 2019; Leceta, Guerrero, & de la Caba, 2013a; Li et al., 2014). All these parameters should be taken into account to choose the better film formulation that gives good barrier properties against light and water, mechanical resistance and biological activities. Further, in order to enhance chitosan film characteristics several chemical, physical and enzymatic modifications methods were envisaged to enlarge their domain of applications including Maillard reaction (MR), heat treatment and the combination of two polymers (Affes et al., 2020c; Fernández-de Castro et al., 2016; Gullón et al., 2016; Hajji et al., 2018; Leceta, Guerrero, Ibarburu, Dueñas, & de la Caba, 2013b). Given

4

the good antioxidant and antibacterial activities of MR products (MRP) in food industry, their use as preservatives is attracting increasing interest (Gullón et al., 2016; Hamdi et al., 2020).

Maillard reaction is a non-enzymatic crosslinking complex biochemical process, which is done by heat treatment of amino acids in the presence of reducing sugars, and that produces fluorescent, brown final MRP named melanoidins with high biological properties (Affes et al., 2020c; Etxabide, Urdanpilleta, Gómez-Arriaran, de la Caba, & Guerrero, 2017; Sun et al., 2017; Li et al., 2014). Three stages in the MR are usually considered. The initial products are called Schiff bases. They form Amadori products via rearrangement, which undergo further reactions to form irreversible advanced glycation end products (Kchaou et al., 2018). Having amino groups makes chitosan a candidate to react with the carbonyl group of reducing sugars, and allows it to participate in the MR (Gullón et al., 2016; Li et al., 2014). The rate of this chemical reaction is influenced by many factors, including the type, the concentration and the ratio of carbonyl/amino groups, pH, temperature, time of exposure and water activity (Hamdi et al., 2020; Kchaou et al., 2018; Kchaou et al., 2019; Gullón et al., 2016; Xu, Huang, Xu, Liu, & Xiao, 2019).

In a previous study (Affes et al., 2020c), the factor amino-containing compound was investigated using chitosan and high Mw-chitosan-depolymerization-products (CDP) (1244.7, 482.03 and 163.56 kDa), while maintaining constant the same added-carbonyl-containing compound, which is glucose at a concentration of 0.5 mg/ml, in all films' formulations. Changes undergone by crosslinking and MR development, after heat-treatment during 24 h at 90 °C, demonstrated better functional, thermal and mechanical properties in higher Mw chitosan-based films. Although many studies, dealing with MR crosslinked-chitosan-based films, have been achieved and the factors affecting the reaction, including characteristics (Mw and AD of chitosan) and concentration of amino groups donors, pH and water activity, have been evaluated, there are no many previous reports on the effect of the others factors, particularly the

nature of reducing sugars (Fernández-de Castro et al., 2016; Gullón et al., 2016; Kosaraju et al., 2010; Li et al., 2014). Thus, in the present work, chitosan was used as constant amino-containing compound and other parameters affecting MR development were studied.

The present research aims to evaluate the effects of different heating conditions, including temperature and incubation time, and types of reducing sugars (glucose and different low molecular weight (Mw) chito-oligosaccharides (COS) with varying acetylation degree (AD)), at a concentration of 5 mg/ml, on the extent of MR on chitosan-based films. To this end, chitosan, chitosan/glucose and chitosan/COS-based films were thermally treated at 90 and 110 °C and for 6 and 24 h and their functional, structural, thermal, mechanical and antioxidant properties were compared.

To the best of our knowledge, this is the first study dealing with the use of low-Mw COS, having different acetylation degree, as carbonyl-containing compounds, to develop MR on chitosan-based films, to optimize films crosslinking conditions, as well as to correlate MR rate with resulted films physico-chemical and antioxidant properties.

2. Materials and methods

2.1. Materials

Shrimp chitosan (Ch) (Molecular weight (Mw), 1244.70 kDa; Acetylation degree (AD), 7.60 ± 0.54%) was prepared as described in our previous study (Affes et al., 2019) and employed as filmogenic biopolymer for films preparation. Two different chito-oligosaccharides (COS) were prepared by chitosan hydrolysis during 24 h using the chitosanolytic crude extract from *Portunus segnis* blue crab viscera (pH 4.0, 40 °C and E/S ratio = 100 U/g chitosan) (Affes et al., 2019) and the chitosanolytic preparation from *Bacillus licheniformis* strain (pH 5.0, 50 °C and E/S ratio = 70 U/g chitosan) (Affes et al., 2020b), respectively. The mixtures chitosan/chitosanases were incubated at appropriate conditions and the obtained soluble parts

were freeze-dried, characterized by using steric exclusion chromatography (SEC-HPLC) and the first derivative Ultraviolet (UV) spectrophotometric method and referred as COS1 (Mw, < 4.4 kDa; AD, 18.20 ± 1.19%) and COS2 (Mw, < 4.4 kDa; AD, 10.63 ± 0.17%) using the digestive and bacterial chitosanases, respectively.

COS1, COS2 and D (+) anhydrous-glucose (Glu) ($C_6H_{12}O_6$; 180 g mol^{-1}) were used as reducing sugars to initiate the Maillard Reaction (MR) in chitosan-based films. Anydrous glycerol was purchased from Fluka (98% purity, Fluka Chemical, Germany) and used as plasticizer for the films. All other reagents were of analytic grade.

2.2. Films preparation

Films forming solutions (FFS) were prepared by dissolving chitosan (10 mg/ml) in acetic acid (1%, v/v). Then, three categories of films were prepared by the addition of three different reducing sugars to promote MR development; glucose, COS1 and COS2, at a concentration of 5 mg/ml. Glycerol was added as a plasticizer to the solutions at a concentration of 15% (w/w dry chitosan matter) and the FFS were maintained under stirring for 30 min. Subsequently, a volume of 34.0 ml of each FFS was cast in Polystyrene Petri dishes (13.5 x 13.5 cm diameter) and left to dry for 48 h at 25 °C. Dried films were manually peeled off from the surface and non-heated films were considered as blank and referred as F1 (Ch), F2 (Ch-Glu), F3 (Ch-COS1) and F4 (Ch-COS2).

All prepared films were then conditioned at 25 °C and 50% relative humidity (RH) before analyses, except for Fourier-transform infrared spectroscopy (FTIR), X-ray diffraction (XRD) and thermogravimetric analyses (TGA), films were equilibrated at 0% RH.

2.3. Heating treatment of films

Then, to induce MR, the films (with or without reducing sugar) were heated in an oven at two different temperatures (90 ± 2 and 110 ± 2 °C) and for different incubation times (6 and

167   24 h). The films heated at 90 °C during 6 and 24 h were named F1-90-6 h, F1-90-24 h, F2-90-

168   6 h, F2-90-24 h, F3-90-6 h, F3-90-24 h, F4-90-6 h and F4-90-24h, respectively for F1, F2, F3

169   and F4. While, the films heated at 110 °C were named F1-110-6 h, F1-110-24 h, F2-110-6 h,

170   F2-110-24 h, F3-110-6 h, F3-110-24 h, F4-110-6 h and F4-110-24h for F1, F2, F3 and F4

171   respectively.

2.4.   Physicochemical characterization of the films

2.4.1.   Color properties

Color development was studied using a CIE colorimeter (CR-5, Konica Minolta, Sensing Europe B.V). Color of the films was expressed as L* (lightness/brightness), a* (greenness/ redness) and b* (blueness/yellowness). The total color change (ΔE^*) of the films was determined as follows:

$$\Delta E = \sqrt{((L^* - L_0^*)^2 + (a^* - a_0^*)^2 + (b^* - b_0^*)^2)} \qquad \textbf{Eq. (1)}$$

where L_0^*, a_0^*, b_0^* are the colorimetric parameters of the film F1, as standard, and L*, a*, b* are the values of the modified films.

The obtained CIE Lab values were then used to calculate the browning index (BI) as mentionned in equation 2:

$$BI = \frac{(100 \times (z - 0.31))}{0.172} \quad \text{with} \quad z = \frac{a^* + 1.75\,(L^*)}{5.645\,(L^*) + (a^*) - 3.012\,(b^*)} \qquad \textbf{Eq. (2)}$$

2.4.2.   UV-visible light spectroscopy

The films were cut into rectangles (1.0 x 3.0 cm) and placed in the test cell of an UV-visible (UV-vis) spectrophotometer (Shimadzu UV-2401PC). Light transmission of the films was determined in the wavelength range from 200 to 800 nm. An empty test cell was used as a reference.

2.4.3.   FTIR-ATR analysis

8

190 FTIR spectra of the studied films were assessed using a spectrometer (Agilent

191 Technologies, Cary 630 series) equipped with an attenuated reflection accessory (ATR)

192 containing a diamond/ZnSe crystal, at 25 °C. Data analysis and treatment was carried out by

193 using the OMNIC spectra software (Thermo Fisher Scientific).

194 **2.4.4. Water content and solubility**

195 The water content (WC) of the films (g $_{moisture}$/100 g $_{film}$), was determined by measuring

196 the weight loss of each film sample (100 mg) after drying in an oven at 105 °C until constant

197 weight was reached according to the following equation:

198
$$WC\ (\%) = \frac{(m_i - m_f)}{m_i} \times 100 \qquad \textbf{Eq. (3)}$$

199 where m_i is the initial film weight (g) and m_f is the final is the final film dry weight (g). Three

200 samples of each formulation were analyzed.

201 The solubility of the films in water (WS) was studied according to the Gennadios et al.

202 (1998) method. WS was calculated as follows:

203
$$WS\ (\%) = \frac{[(m_i \times (100 - MC)) - m_f]}{(m_i \times (100 - MC))} \times 100 \qquad \textbf{Eq. (4)}$$

204 where m_i is the initial film weight (g), m_f is the final dry film weight (g) and WC is the water

205 content of each film sample (%). All tests were carried out in triplicate.

206 **2.4.5. Water contact angle**

207 The contact angle measurements were measured using the sessile drop method on a GBX

208 equipment (Digidrop, Romans, France), equipped with an image analysis software (Visiodrop).

209 Six measurements per films were carried out. All the tests were conducted in an environmental

210 chamber at 25 (± 2) °C and with a relative humidity of 50 (± 1) %.

211 **2.4.6. Film thickness**

9

Film thickness was measured using a micrometer (Digimatic IP65, Mitutoyo, France). Six measurements at different positions were done for each film sample. The mean value was taken into account for mechanical properties parameters calculation.

2.4.7. Mechanical properties

Tensile strength (TS, MPa) and elongation at break (EAB, %) of the films were determined using a rheometer apparatus (Physica MCR, Anton Paar, GmbH, France) equipped with a mechanical properties measuring geometry. Rheoplus software was used for the estimation of TS and EAB, corresponding respectively to the maximum load and the final extension at break from the tensile stress *vs.* strain curves. Six measurements for each films formulation were carried out at 25 °C.

2.4.8. Thermal stability analysis

The thermal stability of the film was studied, at a temperature range from 30 to 600 °C, using a thermogravimetric analysis (TGA, Q500 High Resolution, TA Istruments). The temperature of maximum degradation (T_{max}, °C), the weight loss (Δw, %) and final residue at 600 °C (%) values were determined using TA Universal Analysis 2000 software (Version 4.5 A, TA instruments).

2.4.9. X-ray diffraction analysis

The crystallinity of the selected films was performed by x-ray diffraction analysis, at 2θ from 7 to 40 °, using a Philips diffractometer equipped with monochromatic Cu K_α radiation source.

2.4.10. Films microstructure

The microstructure of the films was assessed by surface and cross-section observations using a scanning electron microscopy (SEM, Hitachi S4800), at different magnifications.

2.5. Antioxidant activity

The capacity of film samples (10 mg) to scavenge 2,2′-Azino-bis (3-ethylbenzothiazoline-6-sulfonic acid) ($ABTS^+$) and 1,1-diphenyl-2-picrylhydrazyl (DPPH) radicals was studied according to the methods of Re et al. (1999) and Bersuder, Hole, & Smith (1998), respectively. The absorbances of the final solutions were mesured at 734 and 517 nm, after 10 min and 24 h of incubation in the dark, respectively for DPPH and ABTS scavenging activity.

The ability of films (10 mg) to reduce iron (III) was evaluated according to the method described by Yidirim, Mavi, & Kara (2001) with slight modification of the incubation time at 50 °C during 3 h. The absorbance of the final solutions was measured at 700 nm.

The total antioxidant ability of the films (10 mg) to reduce Mo (VI) to Mo (V) and to form a green phosphate/Mo (V) complex at acidic pH was studied as reported by Prieto, Pineda, & Aguilar, (1999). The absorbance was measured at 695 nm. All the experiments were carried out in triplicate.

2.6. Statistical analysis

Statistical analyses were performed with IBM SPSS Statistics v.20. Normal distribution and equality of variance were tested with the Shapiro-Wilk and Levene's tests respectively. Statistically significant differences were then calculated using the Kruskal-Wallis test for non-normal distributed data with the dunn's post hoc test. Differences were considered significant at $p \ value$ < 0.05. Standard deviation errors were used to compare all experiments.

3. Results and discussion

3.1. Effect of Maillard reaction on films optical and spectral properties

3.1.1. Films color change

11

258   To evaluate the effect of MR on chitosan-based films, different reducing sugars including

259   glucose and chito-oligosaccharides (COS1 and COS2) were added to the FFS. Films were

260   incubated at 90 and 110 °C for 0, 6 and 24 h to perform MR. During reaction, reducing sugars

261   reacted with amino acid residues of chitosan to form the final MR products (MRP). The final

262   stage of MR was evaluated by color change measurement. Films color was measured using

263   CIELab   scale   and   L*   (darkness/whiteness),   a*   (greenness/redness)   and   b*

264   (blueness/yellowness) parameters were used to calculate difference in color (ΔE^*) and

265   browning index (BI).

266   Results illustrated in **Table 1** showed that L* values of the control unheated films F1, F3

267   and F4 are similar ($p > 0.05$). However, it decreased significantly in the film F2 containing

268   glucose (Glu). Further, after thermal treatment of the films, L* values decreased significantly

269   indicating that these films turn darker. For all the formulations, this decrease was more

270   noticeable after heating at 110 °C, as compared to 90 °C and after incubation time during 24 h

271   in comparison with those incubated for 6 h. Furthermore, the decrease of L* values was more

272   pronounced in the films containing glucose followed by the films containing COS1 and COS2

273   as compared to the films of chitosan. After heating at 90 °C, there are no significant decrease

274   in L* values of chitosan films without reducing sugar, however, negligible change of L* values

275   was observed after heating at 110 °C. Darker color of the films indicate the development of

276   MR, due to the interaction between chitosan and reducing sugars (Glu or COS), allowing to the

277   production of dark MRP. These brown products produced during the final stage of MR are

278   melanoidins (Affes et al., 2020c).

279   Interestingly, thermal treatment of all the films decreased their a* values and increased

280   their b* values, as compared to the control unheated films, turning to green and yellow color

281   region, respectively ($p < 0.05$). These variations were more significantly pronounced as

282 temperature and heating time increased and in the films containing glucose followed by the

283 films containing COS1 and COS2 as compared to chitosan films.

284   Moreover, ΔE^* values, obtained by comparing the color of the films with the film F1,

285 showed a slight difference between the control films more pronounced in the film F2 (3.6 $\pm$

286 0.90). However, a high significant change of color was obtained in the MR-crosslinked films,

287 which is correlated with the increase of the heating time and temperature and differed toward

288 the used reducing sugar. Indeed, this effect was highest at 110 °C and after 24 h of treatment

289 and when glucose was added as reducing sugar (18.80 $\pm$ 0.22), followed by COS1 (11.30 $\pm$

290 0.34) and COS2 (8.34 $\pm$ 0.36) comparing to chitosan film (4.20 $\pm$ 0.34).

291   Besides, the BI, which give an overall evaluation of the progress of the MR according to

292 the development of colored compounds, was measured and results are illustrated in **Table 1**. In

293 all the heated films, the BI values were higher as temperature and incubation time were higher.

294 Further, low BI values were obtained in the treated free-reducing sugar chitosan-based films

295 (2.30 $\pm$ 0.39 for F1-110-24 h). However, similarly to the trend of ΔE, the BI of heated films

296 conjugated with Glu (120.85 $\pm$ 5.27 for F2-110-24 h) was higher than that of chitosan/COS1

297 (33.79 $\pm$ 0.91 for F3-110-24 h) and chitosan/COS2 films (18.01 $\pm$ 1.87 for F4-110-24 h).

298   All of these results indicates that MR was more pronounced for chitosan/Glu films

299 followed by chitosan/COS1 and chitosan/COS2 films, comparing with chitosan film, as

300 evidenced by the intensity of the change of color to dark-yellowish. This fact could indicate

301 that severer reactions occurred in the chitosan films conjugated with Glu than in the films

302 containing COS, allowing to the generation of higher amount of melanoidins. Similarly, Xu et

303 al. (2019) illustrated that milder color change was obtained for soybean protein isolate (SPI)

304 films conjugated with COS as compared to Glu, implying that COS was less susceptible to the

305 MR with SPI than Glu. Moreover, it appeared that color change was higher in the films

306 containing COS1 than those containing COS2, this fact can be attributed to the difference in

13

307 depolymerisation degree (DP) allowed by the different method of chitosan depolymerization

308 despite the higher AD of COS1 (18.20%) than COS2 (10.63%).

309 Furthermore, results demonstrate that the development of MR was more significant when

310 temperature and heating time increased. In this context, Leceta et al. (2013a) reported that color

311 parameters changed notably for chitosan-based films after being heat-treated at 105 °C for 24

312 h, which could mean that the film structure changed. Kchaou et al. (2019) reported that the

313 color change of heated gelatin-glucose films increased as a function of heating temperature

314 indicating better extent of MR of these films at higher temperature. Further, Etxabide et al.

315 (2015) and Kchaou et al. (2018) proved that color change of gelatin-lactose and gelatin-glucose

316 films, respectively, was more pronounced as heating time increased, turning toward dark yellow

317 at longer times, due to the production of higher amount of brown melanoidins (Affes et al.,

318 2020c). Darker films, generated after MR development, have stronger barrier ability in the

319 visible region and are advantageous to prevent oxidative deterioration by coating sensitive to

320 light foods (Yang et al., 2015).

321 **3.1.2.   Ultraviolet-visible (UV-vis) spectroscopy**

322 UV-vis spectroscopy was carried out in the range 200-800 nm in order to analyze the

323 effect of crosslinking as a function of heating time and temperature and using different reducing

324 sugars. Spectra, presented in **Fig. 1A, 1B, 1C, 1D**, showed that the control unheated films had

325 poor barrier properties to light in the UV region, being the preventive effect slightly better for

326 films conjugated with reducing sugars, particularly with glucose.

327 Further, as can be seen, the absorbance of all the heated films highly increased as function

328 of temperature and heating time. Interestingly, in all cases, the absorbance was higher when the

329 films were heated at 110 °C than 90 °C and after 24 h of reaction time than 6 h. Indeed, the

330 conditions 110 °C - 24 h were more efficient than 110 °C - 6 h followed by 90 °C - 24 h and 90

331 °C - 6 h to develop high UV absorbance compounds. Furthermore, when chitosan films without

14

reducing sugar were heated a slight increase was obtained, mainly after heating at 110 °C, as compared to F1. This modification was attributed to the caramelisation reaction due to heating of chitosan (Li et al., 2014). Moreover, there was a sharp increase in absorbance (A) in the range of 200 – 500 nm for the heated films F2, F3 and F4, as compared to the control unheated films. This increase was clearly higher in the films F2 conjugated with Glu followed by the films containing COS1 and the films conjugated with COS2. These results are in line with the color change.

The concomitant rise of absorption of the heated films containing reducing sugars indicate the formation of MRP generated by the development of MR, which is a condensation reaction between nitrogen-containing compounds of chitosan and carbonyl group of reducing sugars (Li et al., 2014). The interactions between functional amino and carbonyl groups, present in chitosan and glucose or COS, respectively, are associated to the development of intermediate colorless compounds (Amadori) absorbing at 294 nm, prior to the generation of brown pigments (melanoidins), absorbing at 420 nm, as final MRP (Kchaou et al., 2018; Gullón et al., 2016). Results showed that in all cases, the values of absorbance at 294 nm ($A_{294\,nm}$) were significantly higher than those obtained at 420 nm ($A_{420\,nm}$). Similarly, Kosaraju, Weerakkody, & Augustin, (2010) proved that the thermal treatment of chitosan with the addition of glucose found higher rates of intermediate browning products than final browning products. In addition, they were greater when temperature and heating time were higher. Moreover, the absorbance at 280 and 420 nm of the heated films conjugated with glucose were higher than those of the heated films containing COS1 and COS2 comparing to heated chitosan films. This means much more intermediate compounds of the MR and darker color. These results indicated that temperature, incubation time and the type of reducing sugar affected crosslinking by MR extension. In the same context, Gullón et al. (2016) reported that reaction conditions, especially temperature and reaction time, affect the formation of chitosan/glucose derivatives by MR.

3.1.3. Fourier-transform infrared spectroscopy (FTIR)

Chemical changes of chitosan film structure, due to reducing sugars addition and MR development at different heating times and temperatures, were studied using FTIR spectroscopy. FTIR spectra presented in **Fig. 2A, 2B, 2C, 2D** showed that similar characteristic peaks were obtained for all the films. All films spectra revealed the presence of the stretching vibrations of hydroxyl group (O-H), CH_2 and CH_3 groups, amide I (C=O in the NH-COCH$_3$ group), amide II (N-H) and C-H bending vibration of CH_2 groups obtained at 3370, 2875, 1630, 1550, and 1450 cm^{-1}, respectively. These three latter absorption bands showed a shift to a lower wavenumber as compared to chitosan powder, which were 1650, 1562 and 1420 cm^{-1}, respectively as described in our previous study (Affes et al., 2019). This shift was due to the relaxation of the chains additionally to the effect of glycerol addition and its interaction with chitosan (Affes et al., 2020a ; Fernández-de Castro et al., 2016). Furthermore, for the control films, the intensity of the N-H band obtained at 1550 cm^{-1} was higher than the intensity of the band of the carbonyl groups C=O at 1630 cm^{-1}. The higher intensity of the amine groups is a result of the presence of activated amine groups ($-NH_3^+$) generated during the films evaporation (Fernández-de Castro et al., 2016).

Furthermore, small shifts of the amide I and amide II peaks from 1630 and 1550 cm^{-1} to around 1615 and 1536 cm^{-1}, respectively, were observed for all MR-crosslinked films. Indeed, the shift of the absorption peak of the Amide I to 1615 cm^{-1} suggests the formation of Schiff base (C=N) between the reducing sugar termination and the chitosan amino groups (Affes et al., 2020c ; Kchaou et al., 2018). The shift of the characteristic peak of the Amide II of MR-crosslinked films was ascribed to the chitosan conformational transformations occurring during the crosslinking reaction between chitosan and reducing sugars.

Nevertheless, after thermal treatment of all the films, the intensity of the different bands of the spectra decreased as compared to unheated films. This decrease was more pronounced in

382　the films containing glucose, especially F2-110-24 h, and when the films were heated during

383　higher time (24 h) and at higher temperature (110 °C). These results were in accordance with

384　WS values variation between control and heated films. As well, the difference in the intensity

385　between the 1630 and 1550 cm^{-1} absorption bands became smaller. Similarly, Gullón et al.

386　(2016) stated that the intensity of chitosan polymer powder decreased after thermal treatment

387　at 60 °C during 32 h.

388　　　All these results proved the crosslinking of the films due to MR development between

389　carbonyl and amine groups thanks to heating treatment. This reaction was more noticeable when

390　reducing sugars were added, especially glucose. These results corroborate with the study of

391　Fernández-de Castro et al. (2016) for heated chitosan and chitosan/COS films. Leceta et al.

392　(2013b) demonstrated also the change in the chemical structure of chitosan films after heat

393　treatment by FTIR spectra variation analysis.

394　**3.2.　Water resistance features of chitosan based films modified by MR**

395　　　Water sensitivity of the films, which is an important factor in the shelf life of packaging

396　materials, was studied by measurement of moisture content (WC), water solubility (WS) and

397　water contact angle (WCA).

398　　　Results illustrated in **Table 2** showed that WC values of the control unheated films

399　containing glucose (14.07%), COS1 (13.98%) and COS2 (14.15%) were significantly higher

400　than WC value of chitosan film (12.28%). This is probably due to the humectant character of

401　glucose and to the WC of COS1 and COS2. Additionally, the heat treatment of the different

402　films proved a high decrease of WC values as compared to the control films. This decrease was

403　higher as the temperature and the heating time were higher ($p < 0.05$). Indeed, heating

404　conditions of 110 °C for 24 h showed the lowest WC values followed by 110 °C-6 h, 90 °C-24

405　h and 90 °C-6 h, for all the films. Furthermore, the highest WC decrease was observed in the

406　heated films containing glucose, especially F2-110-24 h (from 14.07 to 9.60%). The decrease

407   of WC by thermal treatment is due to the interaction between the amino group of chitosan and

408   the carbonyl group of the different reducing sugars (glucose, COS1 or COS2) through MR.

409   Similarly, Kchaou et al. (2018) reported that WC values of gelatin films increased with the

410   addition of glucose and decreased gradually after heating at 90 °C with heating time and glucose

411   content. Rivero, García, & Pinotti (2012) stated that heating of chitosan film at 100, 160 and

412   180 °C decreased its moisture content value which is lower at higher temperature.

413   In addition to its importance to assess the extension of MR, it is crucial to control film

414   solubility to be applied as food coatings, allowing several potential benefits. To this end, films

415   WS was evaluated. As shown in **Table 2**, the addition of glucose, COS1 and COS2 to control

416   unheated chitosan film lead to a significant increase of its WS from 12.12% to 16.19, 18.56 and

417   19.00%, respectively. The higher WS of chitosan/COS films is due to the total water solubility

418   of the added COS as described in our previous studies (Affes et al., 2019; Affes et al., 2020b).

419   Contrarily, when the films were heat-treated, WS values decreased significantly, as

420   compared to unheated films, and proportionally to the increase of temperature and heating time

421   indicating a change in the chemical structure of the films by thermal treatment. The high

422   decrease of WS values in the films containing reducing sugars, especially in the films

423   containing glucose, is due to the development of interactions between amino and carbonyl

424   groups of chitosan and reducing sugars, respectively, induced by temperature, allowing to the

425   crosslink of the films through MR. The decrease of free amino groups in film matrix lead to

426   obtain more compact structure less sensitive to water with WS values (Umemura & Kawai,

427   2007). Likewise, Fernández-de Castro et al. (2016) proved that chitosan/oligosaccharide film

428   showed higher WS value than chitosan film and that thermal treatment at 105 °C decreased

429   significantly WS by the development of brown compounds through MR. In addition, Umemura

430   & Kawai (2007) stated that the solubility in acetic acid of chitosan films conjugated with

431   glucose and cellobiose decreased after thermal treatment at 50 °C for 15 h. In this context,

432   Etxabide et al. (2015) reported that the WS of gelatin films decreased with the addition of

433   lactose and that this reduction of WS is more pronounced at higher concentrations of lactose

434   and after treatment at 105 °C for longer time.

435   Water contact angle (WCA) values are considered as a good indicators of the degree of

436   hydrophilicity of the film surface, being higher when hydrophilicity is lower. The final state of

437   a water drop informs about the surface wettability (Leceta et al., 2013a). The surface properties

438   of the films were evaluated by WCA measurements. Results depicted in **Table 2** showed the

439   variation of WCA of chitosan films as a function of temperature, heating time and type of

440   reducing sugars. WCA values slightly decreased after 20 s (T_{20s}) of depositing the drop as

441   compared to 10 s (T_{10s}), due to water evaporation. Additionally, control chitosan film (F1)

442   showed the higher WCA values. However, the addition of glucose (85.09 °), COS1 (65.50 °)

443   and COS2 (59.20 °) to chitosan films decreased significantly the WCA as compared to F1. The

444   hydrophilicity of these latter films was probably attributed to their higher WC that make them

445   more susceptible to absorb water molecules. After thermal treatment, WCA regress

446   significantly for all the films as compared to the unheated ones indicating that heating leads to

447   an increase of films hydrophilicity as a result of Maillard crosslinking reactions. This reduction

448   was more important when temperature and heating time were higher. Further, control and

449   heated chitosan-based films without reducing sugar addition were considered as hydrophobic

450   films as they exhibit WCA values higher than 90 °. Similarly, Kchaou et al. (2018) stated that

451   WCA of gelatin-glucose films decreased after thermal treatment at 90 °C as a function of

452   heating time. Furthermore, Leceta et al. (2013b) proved that the heat-treatment of chitosan films

453   containing 15% glycerol for 24 h at 105 °C caused a slight decrease in WCA values as compared

454   to un-heated films.

455   **3.3. Thickness and mechanical properties changes of MR treated chitosan-based films**

Results from **Table 2** show that overall films possess similar thickness of approximately 31.0 μm ($p > 0.05$). The mechanical properties, including tensile strenght (TS) and elongation at break (EAB), of the different films were measured and displayed in **Table 2**, except for the heated films containing glucose because they were too brittle to be tested.

Based on the tensile stress *vs.* strain curves, TS and EAB values of chitosan-based film showed slight non-significant decrease when glucose was added to the control film F2. This decrease was probably attributed to the high concentration of glucose (5 mg/ml) incorporated in the film. Heating of this films generate slightly more tearable and brittle films, with not significant differences. Similarly, Hamdi et al. (2020) demonstrated that no significant effect on mechanical properties of control chitosan film was obtained with the addition of glucose, at a concentration of 0.4 mg/ml, and that heating of chitosan/glucose film increase its mechanical behavior.

In addition, a non-significant decrease of TS and EAB was obtained with the addition of COS1 and COS2 for the control films F3 and F4. Further, mechanical parameters values of the film F4 were slightly higher than F3. This variation can be explained by the higher AD of COS1 (18.20%) than COS2 (10.63%). Similarly, Hamdi et al. (2019) reported that AD influences chitosan film-forming mechanical properties and that lower AD chitosan provides better film mechanical behavior.

Moreover, heat treatment of chitosan, chitosan/COS1 and chitosan/COS2 films slightly improve their mechanical properties. The film F3-110-24 h showed the highest increase of EAB as compared to F3 and the film F1-110-24 h showed the highest TS value ($p < 0.05$). Further, this increase of mechanical properties values was correlated with the thermal treatment conditions in the following order of reactivity: 110 °C-24 h > 110 °C-6 h > 90 °C-24 h > 90 °C-6h. Thus suggesting that higher temperature and heating time were more efficient to obtain more flexible and stretchable chitosan and chitosan/COS films.

481   The slight enhancement of mechanical properties of chitosan films by heating treatment,

482   especially for F1-110-24 h, is an accordance with results obtained by Leceta et al. (2013b) who

483   demonstrated that heating of chitosan film at 105 °C for 24 h increased its TS and EAB values.

484   Moreover, these results were in agreement on with those of Hamdi et al. (2020) who stated that

485   heat treatment at 90 °C for 24 h did not affect significantly the mechanical parameters of

486   chitosan blank film. The better flexibility and stretchability of heated films as compared to

487   control films was attributed to the formation of more compact network through MR crosslinking

488   (Park et al., 1999).

3.4. Thermal properties of MR crosslinked chitosan-based films

490   The thermal stability was assessed by means of thermogravimetric analysis (TGA), in a

491   range of temperature between 30 and 600 °C, in order to study the changes occurred by the

492   effect of different heating conditions on chitosan-based films with and without reducing sugars

493   addition. The thermal decomposition data in terms of corresponding weight loss (Δw),

494   temperature of maximium degradation (T_{max}) and final residual mass (R) of the films, measured

495   from the curve of the derivate weight loss as fonction of temperature as shown in **Fig. 1E, 1F,**

496   **1G, 1H**, are detailed in **Table S1**.

497   On the TGA derivate weight curves of the control chitosan-based films F1, F2, F3 and F4

498   three transformation steps corresponding to the main stages of weight loss were distinguished.

499   The first stage of transformation (Δw_1) observed below 100 °C is related to the loss of free and

500   bound water. Δw_1 values increased for the chitosan-based films conjugated with reducing

501   sugars F2, F3 and F4 as compared to F1, which is in line with the increase of WC values of

502   these films. Whereas, Δw_1 values of overall heated films decreased comparing to control

503   unheated films. This decrease, that was further correlated with the decrease of WC of heated

504   films, was higher as temperature and heating time were higher.

A second narrow weight loss (Δw_2) appeared at approximatly 140 - 230 °C and was probably attributed to the entrapped water through hydrogen bonds and the elimination reaction of NH_3 as suggested by Martins, Cerqueira, & Vicente (2012) or due to the evaporation of glycerol as considered by Leceta et al. (2013b). Δw_2 values decreased for all the heated films and disappeared for chitosan films containing glucose heated at 110 °C (F2-110-6 h and F2-110-24 h).

The third major stage of weight loss (Δw_3), corresponding to Δw around 44.94 and 57.14%, displayed the degradation or the decomposition of chitosan and COS chains and were higher for heated films comparing to control films (Martins et al., 2012).

Regarding T_{max} values, no change was noted for the film F2 incorporated with glucose (300 °C) as compared to F1 (297 °C). However, the addition of COS to control chitosan-based films decreased their T_{max} values, that were 277.3 and 267 °C for F3 and F4, respectively. After thermal treatment, T_{max} values of all heated films increased as compared to unheated films. This increase was more pronounced when the films were heated at 110 °C comparing to 90 °C and during 24 h as compared to 6 h. When comparing to the chitosan heated films, glucose incorporation increased T_{max} values of heated films, however, T_{max} values of chitosan films conjugated with COS remains lower despite having increased. Similarly, the residual weight at 600 °C (R) was higher for all the heated films as compared to unheated films.

These variations of thermal stability behavior were attributed to the different extent of MR crosslinking, through creation of new bonds in film matrix, between the different films formulations and the different heating conditions. The increase of thermal stability of heated chitosan films containing reducing sugars is explained by the development MRP which could interact with chitosan chains to stabilize the film network leading to more thermally stable films with enhanced functional properties (Hamdi et al., 2020; Kchaou et al., 2019; Leceta et al.,

529 2013b). An increase of thermal stability was further stated for heated free-reducing sugars

530 chitosan films by thermal treatment, but in a less extend than for MR.

3.5. Effect of MR crosslinking on the structural properties of chitosan-based films

3.5.1. X-ray diffraction (XRD) analysis

533   XRD analysis is a proven tool to study the changes of the molecular conformation of

534 chitosan-based films acquired by reducing sugar addition and thermal treatment. The XRD

535 patterns of the different films formulations before and after treatment at 90 and 110 °C for 24

536 h, were illustrated in **Fig. 2E, 2F, 2G, 2H**.

537   As shrimp chitosan is a semi-crystalline polysaccharide due to its regular chain it present

538 two peaks at $2\theta = 10$ and $20°$ associated with its hydrated conformation (Affes et al., 2019).

539 Similarly, XRD chromatogram of chitosan film showed that it was in a partially crystalline state

540 and has two main characteristic peaks with a slight shift, at 2θ around 12 and $20°$. Comparably

541 XRD chromatograms were obtained by Chang et al. (2019), Leceta et al. (2013) and Rivero et

542 al. (2012) for chitosan-based films. When glucose was added to chitosan film (F2), the same

543 peaks were observed but with slightly lower intensity as compared to F1. Whereas, it is clearly

544 shown that the addition of COS reduced the crystallization of chitosan films F3 and F4, where

545 the peak at $12°$ disappeared and the intensity of the peak at $20°$ decreased comparing to F1.

546 This change in the crystallinity open the incorporation of COS1 and COS2 was ascribed to the

547 non-crystalline structure of these two chitosan derivatives (Affes et al., 2019; Affes et al.,

548 2020b).

549   After thermal treatment of the different films, the crystallinity decreases remarkably as a

550 function of heating temperature as evidenced in the decrease in the intensity of the peak at 20

551 °. Indeed, films heating at 110 °C provides less crystalline structure than 90 °C. Further, the

552 intensity of this peak (20 °) was lower in the films containing COS followed by glucose

553 containing films, as compared to F1. As well, the peak at 12 ° disappeared in all the heated

23

554 films. Similarly, diffractograms of chitosan films cured at different temperatures showed the

555 disappearance of the peak located at 2 θ = 15 ° and demonstrated that films heating at higher

556 temperature, 160 °C, leads to lower crystallinity than 100 °C (Rivero et al., 2012). Furthermore,

557 Leceta et al. (2013b) stated that chitosan film structure was influenced by the effect of

558 temperature. These results were in contradiction with those of Fernández-de Castro et al. (2016)

559 who stated that chitosan and chitosan/COS (1:1) films heat treated and non-treated showed the

560 same XRD patterns with amorphous behaviour and a single wide diffraction peak at 20.2 °.

561 **3.5.2. Films microstructure**

562 In order to investigate the microstructural modifications in the elaborated chitosan-based

563 films through MR, the final films microstructure was qualitatively visualized by surface

564 electron microscopy (SEM) analysis. Crosslinked films through MR at 110 °C for 24 h were

565 selected for the SEM analysis, and compared with control unheated films, except for heated

566 film containing glucose where the film F1-90-6 h was tested because F1-110-24 h was too brittle

567 and it is difficult to be fixed on SEM support.

568 Characteristic SEM micrographs of surface and cross-sections of films were shown in

569 **Fig. 3**. The surface of all the films was flat, smooth and homogenous without apparent porosity.

570 However, the films F2 and F2-90-6 h showed the appearance of some cracks more pronounced

571 in the heated film F2-90-6 h, due to the addition of glucose (5 mg/ml).

572 Moreover, cross-sectional images of the control films showed compact and homogenous

573 structure without any evidence of irregularities. Further, crosslinking provides and increases of

574 films cross-sections homogeneity and order, except of the film F2-90-6 h were some cracks

575 were visualized. Results were in accordance with mechanical properties values that increased

576 for heated chitosan and chitosan/COS films and decreased for heated chitosan/glucose films.

577 The more compact structure of the heated chitosan and COS films, as compared to control

578 films, was attributed to the crosslinking through MR thanks to the action of temperature leading

24

579 to high interaction between chitosan and COS. Likewise, Fernández-de Castro et al. (2016)

580 reported that chitosan and chitosan/oligosaccharides based films had homogenous

581 microstructure with relatively roughness and that no irregularities, caused by crosslinking

582 through heat treatment at 105 °C overnight, were observed in the heat treated films.

583 However, the less compact structure of heated chitosan/glucose films despite the high

584 extent of MR in this films, was probably attributed to the very high concentration of glucose.

585 Hamdi et al (2020) reported that the incorporation of glucose at concentrations from 0.5 to 2%

586 (w/w chitosan) to chitosan film improves its microstructure.

3.6. Antioxidant property of activated films by Maillard reaction

588 To evaluate the antioxidant activity of blank and MR-crosslinked chitosan-based films

589 and to correlate antioxidant potential to films structural characteristics, differents *in vitro*

590 antioxidant tests were assayed including DPPH and ABTS$^+$ radicals scavenging activities,

591 reducing power test and the total antioxidant activity.

592 As shown in **Fig. 4**, for the four tested mechanisms, chitosan-based film F1 exhibited the

593 lowest antioxidant behavior. The addition of glucose increased slightly the antioxidant activities

594 values of the film F2 ($p < 0.05$). Further, when COS were incorporated in the control films, a

595 significant increase of the antioxidant potential, via the different tests, was noted which is more

596 pronounced for the film F3 than F4. The higher antioxidant activity of the film F3 than F4 was

597 attributed to the better antioxidant activity of COS1 (Mw, < 4.4 kDa; AD, 18.20 ± 1.19%) than

598 COS2 (Mw, < 4.4 kDa; 10.63 ± 0.17%) as shown in our previous studies (Affes et al., 2019;

599 Affes et al., 2020b). Thus can be a result of the difference in the degree of polymerization, ion

600 composition, and the presence of high units of D-glucosamine in the structure of COS1 despite

601 its high AD than COS2 (Anraku et al., 2018; Li, Liu, Xing, Qin, & Li, 2013). Therefore, for the

602 control films, F3 showed the better antioxidant behavior, followed by F4 and F2 as compared

603 to F1.

25

604   Regarding thermally treated films, values were significantly higher in heated films than

605   in the blank films, even by heating of the film F1, due to the development of active MRP. This

606   increase more noticeable after heating at 110 °C for 24 h followed by 110 °C- 6h, 90 °C-24 h

607   and 90 °C-6 h allowing to conclude that heating at higher temperature (110 °C) and incubation

608   times (24 h) generates better antioxidant films. Further, the heated film F1 showed the lowest

609   increase of antioxidant values which is negligible as compared to heated reducing sugar

610   containing films. However, heated glucose containing films, especially F2-110-24 h showed

611   the better increase of antioxidant potential comparing to the blank film F2. In addition, the

612   heated films containing COS1 (F3 group) exhibited the better antioxidant activities, for all the

613   tests, followed by F2 and F4. Where, the film F3-110-24 h reached 100% for ABTS and DPPH

614   radical scavenging activities, 2.44 ± 0.07 for reducing power test and $179,325 \pm 1.65$ α-

615   tocopherol (μmol/ml) for the total antioxidant activity.

616   The antioxidant activity was enhanced subsequently to the development of MR. This

617   increase was directly correlated to the incorporated reducing sugars in the film matrix, the

618   temperature and the heating time. Different mechanisms could explain the antioxidant activity

619   of MRP. The high scavenging activity of crosslinked films could be a result of the reduction of

620   reactive amino groups, through MR development, generating intermediate and final brown

621   melanoidins that were able to donate hydrogen atoms (Akar, Küçük, & Doğan Akar, 2017; Li

622   et al., 2014; Maillard, Billaud, Chow, Ordonaud, & Nicolas, 2007). Moreover, Chen et al.

623   (2019) and Li et al. (2014) reported that primary MRP and finally brown heterocyclic

624   compounds were responsible to the improved reducing power of the MR crosslinked films.

625   Furthermore, Kchaou et al. (2018) suggested that MRP could react with Mo (VI) to convert it

626   to more stable molecules, Mo (V) by donating electrons, in total antioxidant activity test.

627   **4. Conclusion**

628   Different reducing sugars types (glucose and COS), temperature and heating times were

629 studied to induce Maillard reaction (MR) crosslinking of chitosan-based films. The rate of MR

630 was better at higher temperature and exposure times and for glucose containing films, followed

631 by films conjugated by COS1 and COS2, as shown by browning index values, Ultraviolet and

632 Fourier-transform infrared spectra, water resistance properties and thermal stability

633 degradation. However, crosslinked films mechanical properties were enhanced for

634 chitosan/COS films and reduced for chitosan/glucose films, which is correlated with SEM

635 results. Moreover, MR development enhanced significantly the antioxidant potential, via four

636 different mechanisms, of all the crosslinked films as compared to blank films thanks to the

637 formation of highly active MR products. Among all treated films, the most actives were

638 chitosan/COS1 crosslinked films, followed by chitosan/glucose and chitosan/COS2 films.

639 These films possess interesting functional and antioxidant properties that were suitable for food

640 packaging and biomedical applications.

651 ## **References**

652 Affes, S., Aranaz, I., Hamdi, M., Acosta, N., Ghorbel-Bellaaj, O., Heras, Á., Nasri, M., &

653   Maalej, H. (2019). Preparation of a crude chitosanase from blue crab viscera as well as its

654   application in the production of biologically active chito-oligosaccharides from shrimp

655   shells chitosan. *International Journal of biological macromolecules, 15,* 558–569.

656 Affes, S., Maalej, H., Aranaz, I., Acosta, N., Kchaou, H., Heras, Á., & Nasri, M. (2020a).

657   Controlled size green synthesis of bioactive silver nanoparticles assisted by chitosan and

658   its derivatives and their application in biofilm preparation. *Carbohydrate Polymers, 236,*

659   116063.

660 Affes, S., Maalej, H., Aranaz, I., Acosta, N., Heras, Á., & Nasri, M. (2020b). Enzymatic

661   production of low-*Mw* chitosan-derivatives: Characterization and biological activities

662   evaluation. *International Journal of Biological Macromolecules, 144,* 279–288.

663 Affes, S., Nasri, R., Li, S., Van Der Lee, A., Nasri, M., & Maalej, H. (2020c). Effect of glucose-

664   induced Maillard reaction on physical, structural and antioxidant properties of chitosan

665   derivatives-based films. *Carbohydrate Polymers, 255,* 117341.

666 Affes, S., Aranaz, I., Acosta, N., Heras, Á., Nasri, M., & Maalej, H. (2021). Chitosan

667   derivatives-based films as pH-sensitive drug delivery systems with enhanced antioxidant

668   and antibacterial properties. *International Journal of Biological Macromolecules, 182,*

669   730–742.

670 Akar, Z., Küçük, M., & Doğan, H. (2017). A new colorimetric DPPH• scavenging activity

671   method with no need for a spectrophotometer applied on synthetic and natural antioxidants

672   and medicinal herbs. *Journal of Enzyme Inhibition and Medicinal Chemistry, 32,* 640–647.

673 Anraku, M., Gebicki, J. M., Lohara, D., Tomida, H., Uekama, K., Maruyama, T., Hirayama, F.,

674   & Otagiri, M. (2018). Antioxidant activities of chitosans and its derivatives in *in vitro* and

675   *in vivo* studies. *Carbohydrate Polymers, 199,* 141–149.

676 Aranaz, I., Acosta, N., Civera, C., Elorza, B., Mingo, J., Castro, C., de los Llanos, Gandía, M.,

677   & Caballero, A.H. (2018). Cosmetics and Cosmeceutical Applications of Chitin, Chitosan

678   and Their Derivatives. *Polymers, 10,* 213.

679 Bersuder, P., Hole, M., & Smith, G. (1998). Antioxidants from a heated histidine-glucose model

680   system. I: Investigation of the antioxidant role of histidine and isolation of antioxidants by

681   high-performance liquid chromatography. *Journal of the American Oil Chemists' Society,*

682   *75,* 181–187.

683 Chang, W., Liu, F., Sharif, H. R., Huang, Z., Goff, H. D., & Zhong, F. (2019). Preparation of

684   chitosan films by neutralization for improving their preservation effects on chilled meat.

685   *Food Hydrocolloids, 90,* 50–61.

686 Chen, K., Yang, X., Huang, Z., Jia, S., Zhang, Y., Shi, J., Hong, H., Feng, L., & Luo, Y. (2019).

687   Modifcation of gelatin hydrolysates from grass carp (*Ctenopharyngodon idellus*) scales by

688   Maillard reaction: Antioxidant activity and volatile compounds. *Food Chemistry, 295,* 569–

689   578.

690 Etxabide, A., Urdanpilleta, M., Guerrero, P., & de la Caba, K. (2015). Effects of cross-linking

691   in nanostructure and physicochemical properties of fish gelatins for bio-applications.

692   *Reactive and Functional Polymers, 94,* 55–62.

693 Etxabide, A., Urdanpilleta, M., Gómez-Arriaran, I., de la Caba, K., & Guerrero, P. (2017).

694   Effect of pH and lactose on cross-linking extension and structure of fish gelatin films.

695   *Reactive and Functional Polymers, 117,* 140–146.

696 Fernández-de Castro, L., Mengíbar, M., Sánchez, A., Arroyo, L., Villarán, M.C., de Apodaca,

697   E.D., & Heras, Á. (2016). Films of chitosan and chitosan-oligosaccharide neutralized and

698   thermally treated: Effects on its antibacterial and other activities. *LWT - Food Science and*

699   *Technology, 73,* 368–374.

700 Galiano, F., Briceño, K., Marino, T., Molino, A., Christensen, K. V., & Figoli, A. (2018).

701 Advances in biopolymer-based membrane preparation and applications. *Journal of*

702 *Membrane Science, 564,* 562–586.

703 Gennadios, A., Handa, A., Froning, G. W., Weller, C. L., & Hanna, M. A. (1998). Physical

704 properties of egg white-dialdehyde starch films. *Journal of Agricultural and Food*

705 *Chemistry, 46,* 1297–1302.

706 Gullón, B., Montenegro, M. I., Ruiz-Matute, A. I., Cardelle-Cobas, A., Corzo, N., & Pintado,

707 M. E. (2016). Synthesis, optimization and structural characterization of a chitosan-glucose

708 derivative obtained by the Maillard reaction. *Carbohydrate Polymers, 137,* 382–389.

709 Hajji, S., Younes, I., Affes, S., Boufi, S., & Nasri, M. (2018). Optimization of the formulation

710 of chitosan edible coatings supplemented with carotenoproteins and their use for extending

711 strawberries postharvest life. *Food Hydrocolloids, 83,* 375–392.

712 Hamdi, M., Nasri, R., Hajji, S., Nigen, M., Li, S., & Nasri, M. (2019). Acetylation degree, a

713 key parameter modulating chitosan rheological, thermal and film-forming properties. *Food*

714 *Hydrocolloids, 87,* 48–60.

715 Hamdi, M., Nasri, R., Ben Azaza, Y., Li, S., & Nasri, M. (2020). Conception of novel blue crab

716 chitosan films crosslinked with different saccharides via the Maillard reaction with

717 improved functional and biological properties. *Carbohydrate Polymers, 241,* 116303.

718 Kchaou, H., Benbettaïeb, N., Jridi, M., Abdelhedi, O., Karbowiak, T., Brachais, C. H., Léonard,

719 M. L., Debeaufort, F., & Nasri, M. (2018). Enhancement of structural, functional and

720 antioxidant properties of fish gelatin films using Maillard reactions. *Food Hydrocolloids,*

721 *83,* 326–339.

722 Kchaou, H., Benbettaïeb, N., Jridi, M., Nasri, M., & Debeaufort, F. (2019). Influence of

723 Maillard reaction and temperature on functional, structure and bioactive properties of fish

724 gelatin films. *Food Hydrocolloids, 97,* 105196.

725 Kosaraju, S. L., Weerakkody, R., & Augustin, M. A. (2010). Chitosan-glucose conjugates:

726 Influence of extent of Maillard reaction on antioxidant properties. *Journal of Agricultural*

727 *and Food Chemisrty, 58,* 12449–12455.

728 Leceta, I., Guerrero, P., & de la Caba, K. (2013a). Functional properties of chitosan based films.

729 *Carbohydrate Polymers, 93,* 339–346.

730 Leceta, I., Guerrero, P., Ibarburu, I., Dueñas, M. T., & de la Caba, K. (2013b). Characterization

731 and antimicrobial analysis of chitosan-based films. *Journal of Food Engineering, 116,* 889–

732 899.

733 Li, K., Liu, S., Xing, R., Qin, Y., & Li, P. (2013). Preparation, characterization and antioxidant

734 activity of two partially N-acetylated chitotrioses. *Carbohydrate Polymers, 92,* 1730–

735 1736.

736 Li, S. L., Lin, J., & Chen, X. M. (2014). Effect of chitosan molecular weight on the functional

737 properties of chitosan-maltose Maillard reaction products and their application to fresh-

738 cut *Typha latifolia* L. *Carbohydrate Polymers, 102,* 682–690.

739 Liu, J., Sun, L., Xu, W., Wang, Q., Yu, S., & Sun, J. (2019). Current advances and future

740 perspectives of 3D printing natural-derived biopolymers. *Carbohydrate Polymers, 207,*

741 297–316.

742 Martins, J. T., Cerqueira, M. A., & Vicente, A. A. (2012). Influence of α-tocopherol on

743 physicochemical properties of chitosan-based films. *Food Hydrocolloids, 27,* 220–227.

744 Maillard, M. N., Billaud, C., Chow, Y. N., Ordonaud, C., & Nicolas, J. (2007). Free radical

745 scavenging, inhibition of polyphenoloxidase activity and copper chelating properties of

746 model Maillard systems. *LWT-Food Science and Technology, 40,* 1434–1444.

747 Park, H. J., Jung, S. T., Song, J. J., Kang, S. G., Vergano, P. J., & Testin, R. F. (1999).

748 Mechanical and barrier properties of chitosan-based biopolymer film. *Chitin and*

749 *Chitosan Research, 5,* 19–26.

750 Prieto, P., Pineda, M., & Aguilar, M., (1999). Spectrophotometric quantitation of antioxidant

751   capacity through the formation of a phosphomolybdenum complex: Specific application

752   to the determination of Vitamin E. *Analytical Biochemistry, 269,* 337–341.

753 Re, R., Pellegrini, N., Proteggente, A., Pannala, A., Yang, M., & Rice-Evans, C. (1999).

754   Antioxidant activity applying an improved ABTS radical cation decolorization assay.

755   *Free Radical Biology & Medicine, 26,* 1231–1237.

756 Rivero, S., García, M. A., & Pinotti, A. (2012). Heat treatment to modify the structural and

757   physical properties of chitosan-based films. *Journal of Agricultural and Food Chemistry,*

758   *60,* 492–499.

759 Sun, T., Qin, Y., Xu, H., Xie, J., Hu, D., Xue, B., & Hua, X. (2017). Antibacterial activities and

760   preservative effect of chitosan oligosaccharide Maillard reaction products on *Penaeus*

761   *vannamei. International Journal of Biological Macromolecules, 105,* 764–768.

762 Umemura, K., & Kawai, S. (2007). Modification of chitosan by the Maillard reaction using

763   cellulose model compounds. *Carbohydrate Polymers, 68,* 242–248.

764 Xu, Z. Z., Huang, G. Q., Xu, T. C., Liu, L. N., & Xiao, J. X. (2019). Comparative study on the

765   Maillard reaction of chitosan oligosaccharide and glucose with soybean protein isolate.

766   *International Journal of Biological Macromolecules, 131,* 601–607.

767 Yang, H., Li, J. G., Wu, N. F., Fan, M. M., Shen, X. L., Chen, M. T., Jiang, A. M., & Lai, L. S.

768   (2015). Effect of hsian-tsao gum (HG) content upon rheological properties of film-

769   forming solutions (FFS) and physical properties of soy protein/hsian-tsao gum films.

770   *Food Hydrocolloids, 50,* 211–218.

771 Yildirim, A., Mavi, A., & Kara, A. A. (2001). Determination of antioxidant and antimicrobial

772   activities of *Rumex crispus* L. extracts. *Journal of Agricultural and Food Chemistry, 49,*

773   4083–4089.

774

775

776

Conflict of interest

The authors declare that there are no conflicts of interest.

Credit authorship contribution statement

Sawsan Affes: Conceptualization, Methodology, Validation, Formal analysis, Investigation, Writing - Review & Editing.

Hana Maalej: Supervision, Conceptualization, Resources, Writing - Review & Editing.

Suming Li: Project administration, Investigation.

Rania Abdelhedi: Statistical analysis.

Rim Nasri: Project administration, Investigation.

Moncef Nasri: Supervision, Resources, Visualisation, Writing - Review & Editing.

Figures captions

Figure 1: UV-vis spectra and DTGA profiles chitosan-based films, before and after (0, 6 and 24 h) thermal treatment through Maillard reaction at 90 °C and 110 °C, without **(A, E)** and with reducing sugars addition: chitosan-glucose **(B, F)**, chitosan-COS1 **(C, G)** and chitosan-COS2 **(D, H)** based films, respectively.

Figure 2: FTIR spectra of chitosan **(A)** chitosan-glucose **(B)** chitosan-COS1 **(C)** and chitosan-COS2 **(D)** films before and after heating at different heating times and temperatures. X-ray diffractograms of control and MR-treated chitosan-based films, during 24 h at 90 and 110 °C, without **(E)** and with the addition of different reducing sugars: glucose **(F)**, COS1 **(G)** and COS2 **(H)**.

Figure 3: Section and surface SEM micrographs of control films and heated films at 110 °C during 24 h, except of the film F2 which is tested after treatment at 90 °C during 6 h.

Figure 4: Antioxidant activities of chitosan-based films conjugated or not with different reducing sugars through MR, as a function of temperature (90 and 110 °C) and heating time (0, 6, 24 h), by means of ABTS$^+$ **(A)** and DPPH **(B)** radicals-scavenging activities (%), reducing power (OD 700 nm) **(C)** and total antioxidant activity (α-tocopherol (μmol/ml)) **(D)**. Values are means ± standard deviation (n = 3). Means with different letters (A-M) indicate significant difference ($p < 0.05$).

Fig. 1

Fig. 2

Fig. 3

Film	Surface	Section	
F1			
F1-110-24 h			
F2			
F2-90-6 h			
F3			
F3-110-24 h			
F4			
F4-110-24 h			

Fig. 4

Table 1: Color parameters (L*, a* and b*), total color change (ΔE*) and browning index (BI) of the different films.

Films	L*	a*	b*	ΔE*	BI
F1	28.36 ± 1.09 ^{AB}	-0.45 ± 0.05 ^{A}	-0.46 ± 0.07 ^{M}	-	-
F1-90-6 h	27.54 ± 0.43 ^{ABCD}	-0.55 ± 0.02 ^{AB}	0.52 ± 0.01 ^{L}	1.32 ± 0.26 ^{H}	0.40 ± 0.03 ^{H}
F1-90-24 h	27.30 ± 0.85 ^{ABCD}	-0.60 ± 0.03 ^{AB}	0.64 ± 0.04 ^{L}	1.68 ± 0.51 ^{H}	0.70 ± 0.11 ^{H}
F1-110-6 h	26.40 ± 0.82 ^{CDE}	-0.77 ± 0.05 ^{BC}	0.71 ± 0.02 ^{L}	2.35 ± 0.70 ^{H}	0.67 ± 0.23 ^{H}
F1-110-24 h	24.54 ± 0.43 ^{GH}	-0.88 ± 0.02 ^{CD}	1.22 ± 0.12 ^{K}	4.20 ± 0.34 ^{G}	2.30 ± 0.39 ^{H}
F2	25.97 ± 1.33 ^{DEF}	-0.64 ± 0.19 ^{B}	2.03 ± 0.01 ^{J}	3.60 ± 0.90 ^{G}	-
F2-90-6 h	16.93 ± 0.60 ^{J}	-1.11 ± 0.05 ^{EF}	6.20 ± 0.14 ^{D}	13.25 ± 0.58 ^{C}	38.65 ± 2.65 ^{C}
F2-90-24 h	14.88 ± 0.40 ^{K}	-1.29 ± 0.08 ^{FGH}	9.20 ± 0.08 ^{B}	16.61 ± 0.38 ^{B}	81.60 ± 4.03 ^{B}
F2-110-6 h	14.68 ± 0.21 ^{K}	-1.41 ± 0.07 ^{GHI}	9.36 ± 0.14 ^{B}	16.87 ± 0.25 ^{B}	84.94 ± 3.53 ^{B}
F2-110-24 h	12.96 ± 0.16 ^{L}	-1.68 ± 0.08 ^{J}	10.26 ± 0.14 ^{A}	18.80 ± 0.22 ^{A}	120.85 ± 5.27 ^{A}
F3	27.83 ± 0.13 ^{ABC}	-0.95 ± 0.02 ^{DE}	1.41 ± 0.02 ^{K}	2.00 ± 0.09 ^{H}	-
F3-90-6 h	24.78 ± 0.65 ^{EFG}	-1.07 ± 0.05 ^{E}	3.90 ± 0.05 ^{G}	5.68 ± 0.66 ^{F}	13.35 ± 1.70 ^{EF}
F3-90-24 h	22.26 ± 0.20 ^{H}	-1.26 ± 0.04 ^{FG}	5.46 ± 0.04 ^{E}	8.54 ± 0.14 ^{E}	22.77 ± 0.03 ^{D}
F3-110-6 h	22.30 ± 0.07 ^{H}	-1.26 ± 0.01 ^{FG}	5.48 ± 0.01 ^{E}	8.53 ± 0.08 ^{E}	22.85 ± 0.90 ^{D}
F3-110-24 h	19.69 ± 0.47 ^{I}	-1.54 ± 0.03 ^{IJ}	6.70 ± 0.03 ^{C}	11.30 ± 0.34 ^{D}	33.79 ± 0.91 ^{C}
F4	28.68 ± 0.23 ^{A}	-1.35 ± 0.01 ^{GHI}	1.39 ± 0.29 ^{K}	2.10 ± 0.22 ^{H}	-
F4-90-6 h	26.57 ± 0.04 ^{BCD}	-1.39 ± 0.02 ^{GHI}	2.58 ± 0.02 ^{I}	3.65 ± 0.03 ^{G}	5.99 ± 0.15 ^{H}
F4-90-24 h	24.47 ± 0.02 ^{GH}	-1.47 ± 0.01 ^{HI}	3.38 ± 0.36 ^{H}	5.56 ± 0.26 ^{F}	9.84 ± 1.58 ^{FG}
F4-110-6 h	24.16 ± 0.06 ^{G}	-1.47 ± 0.02 ^{HI}	3.42 ± 0.13 ^{H}	5.81 ± 0.13 ^{F}	10.18 ± 0.56 ^{FG}
F4-110-24 h	21.89 ± 0.22 ^{H}	-1.51 ± 0.01 ^{IJ}	4.69 ± 0.31 ^{F}	8.34 ± 0.36 ^{E}	18.01 ± 1.87 ^{DE}

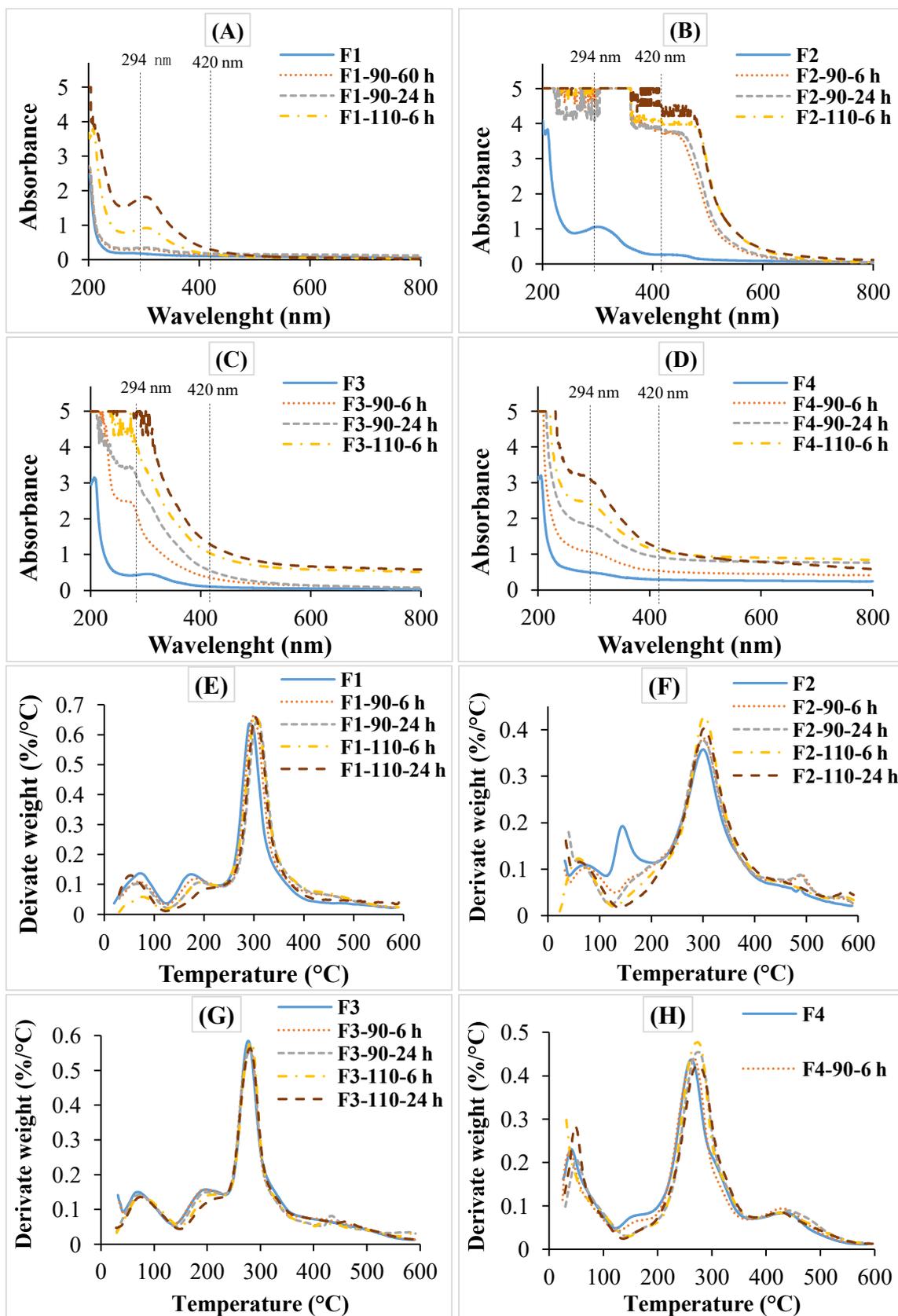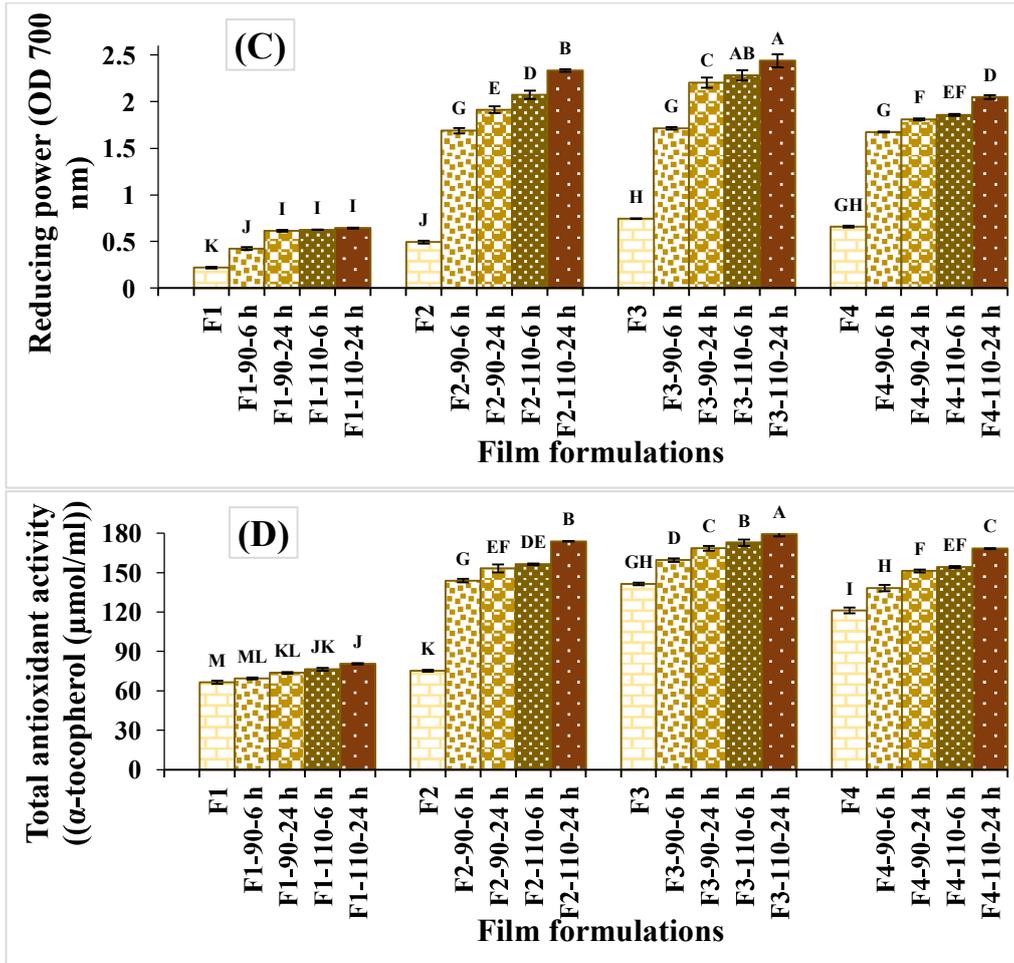Values are means ± standard deviation (n = 3). Means with different letters (A-M) and within a column indicate significant difference ($p < 0.05$). ΔE* was the change of color measured as compared to F1.

Table 2: Water content (WC, %), water solubility (WS, %), water contact angle (WCA, °), thickness (μm) and mechanical properties (TS, % and EAB, MPa) of the different films.

Films	Water resistance properties				Mechanical properties		
	WC (%)	WS (%)	WCA (°)		Thickness (μm)	TS (MPa)	EAB (%)
			$T_{10 s}$	$T_{20 s}$			
F1	12.28 ± 0.16 B	12.12 ± 1.01 CDE	108.60 ± 2.24 A	106.93 ± 2.26 A	29.4 ± 1.5 A	17.99 ± 0.25 A	15.26 ± 0.74 A
F1-90-6 h	10.93 ± 0.23 E	10.71 ± 0.04 HI	96.54 ± 1.78 B	94.18 ± 1.73 B	28.00 ± 2.0 A	18.29 ± 0.01 A	15.35 ± 0.26 A
F1-90-24 h	10.33 ± 0.33 FG	9.33 ± 0.50 JK	95.70 ± 0.62 B	95.10 ± 0.94 B	30.0 ± 4.0 A	18.44 ± 0.73 A	15.50 ± 0.85 A
F1-110-6 h	10.13 ± 0.38 G	8.85 ± 0.27 KL	95.30 ± 1.98 B	94.11 ± 1.77 B	30.0 ± 2.0 A	18.49 ± 0.23 A	15.71 ± 0.12 A
F1-110-24 h	9.31 ± 0.19 H	7.92 ± 0.07 L	94.64 ± 0.67 B	92.93 ± 1.06 B	32.0 ± 4.0 A	18.60 ± 0.30 A	15.93 ± 0.10 A
F2	14.07 ± 0.04 A	16.19 ± 0.32 B	85.09 ± 3.06 C	82.38 ± 3.16 C	30.0 ± 1.5 A	14.05 ± 0.66 A	12.80 ± 0.44 A
F2-90-6 h	11.45 ± 0.16 CD	11.83 ± 0.31 DEFG	71.13 ± 2.07 D	69.19 ± 2.33 D	30.0 ± 3.0 A	-	-
F2-90-24 h	11.06 ± 0.06 DE	11.01 ± 0.09 FGHI	70.49 ± 0.91 D	68.44 ± 0.78 D	31.0 ± 1.2 A	-	-
F2-110-6 h	10.15 ± 0.05 G	10.81 ± 0.22 GHI	69.33 ± 2.15 D	68.24 ± 2.43 D	32.0 ± 5.0 A	-	-
F2-110-24 h	9.60 ± 0.10 H	9.97 ± 0.23 IJ	67.84 ± 0.74 D	66.30 ± 0.80 D	33.0 ± 2.0 A	-	-
F3	13.98 ± 0.08 A	18.56 ± 0.06 A	65.50 ± 2.25 D	58.31 ± 2.46 E	30.0 ± 2.0 A	15.76 ± 0.66 A	14.52 ± 0.1 A
F3-90-6 h	12.60 ± 0.10 B	12.69 ± 0.18 CD	44.81 ± 2.38 F	37.28 ± 1.65 G	30.0 ± 2.0 A	16.83 ± 0.35 A	14.94 ± 0.23 A
F3-90-24 h	11.70 ± 0.10 C	11.97 ± 0.03 CDEF	42.84 ± 1.78 FG	36.69 ± 1.91 GH	31.0 ± 3.0 A	17.19 ± 0.12 A	16.05 ± 0.05 A
F3-110-6 h	11.47 ± 0.04 CD	11.82 ± 0.08 DEFG	39.74 ± 2.59 FG	34.35 ± 2.20 GH	31.0 ± 2.0 A	17.25 ± 0.15 A	16.11 ± 1.40 A
F3-110-24 h	10.75 ± 0.01 EF	11.37 ± 0.54 EFGH	39.74 ± 2.21 FG	33.63 ± 2.96 GH	32.0 ± 4.0 A	17.95 ± 0.64 A	16.64 ± 1.09 A
F4	14.15 ± 0.05 A	19.00 ± 0.23 A	59.20 ± 2.04 E	50.10 ± 2.54 F	32.0 ± 3.0 A	15.95 ± 1.07 A	14.79 ± 0.17 A
F4-90-6 h	12.73 ± 0.03 B	13.01 ± 0.11 C	42.47 ± 2.27 FG	35.05 ± 2.75 GH	32.0 ± 1.0 A	16.09 ± 1.28 A	14.98 ± 0.07 A
F4-90-24 h	11.76 ± 0.04 C	12.24 ± 0.14 CDE	40.93 ± 1.43 FG	34.69 ± 1.24 GH	33.0 ± 2.0 A	16.23 ± 1.20 A	15.29 ± 0.51 A
F4-110-6 h	11.54 ± 0.04 C	12.15 ± 0.25 CDE	38.18 ± 0.89 G	32.45 ± 0.77 GH	34.0 ± 3.0 A	16.49 ± 0.66 A	15.83 ± 0.60 A
F4-110-24 h	10.87 ± 0.10 E	11.91 ± 0.09 DEF	36.82 ± 1.30 G	30.40 ± 0.30 H	34.0 ± 2.0 A	16.87 ± 0.93 A	16.24 ± 0.01 A

Values are means ± standard deviation (n = 3). Means with different letters (A-L) and within a column indicate significant difference ($p < 0.05$).

Supplementary material

Table S1: Maximal degradation temperature (T_{max}, °C), weight loss (Δw, %), and residual weight at 600 °C (R, %) as function of degradation temperatures, based on the TGA thermograms of chitosan based films conjugated or not with glucose and COS through Maillard reaction (MR) at 90 °C and 110 °C and as function of time (0, 6 and 24 h).

Films	T_{max} (°C)	Weight loss (%)			R (%)
		Δw_1	Δw_2	Δw_3	
F1	297.00	9.67	10.6	48.3	31.43
F1-90-6 h	298.09	7.61	10.54	50.57	31.28
F1-90-24 h	298.15	7.20	8.8	51.8	32.20
F1-110-6 h	303.33	7.33	8.06	52.21	32.40
F1-110-24 h	303.50	6.54	6.96	51.49	35.01
F2	300.00	12.18	12.41	44.94	30.47
F2-90-6 h	300.91	8.14	4.20	54.03	33.63
F2-90-24 h	301.00	7.89	4.12	54.52	33.41
F2-110-6 h	301.12	7.74	-	58.14	34.13
F2-110-24 h	301.10	7.35	-	58.03	34.63
F3	277.30	12.56	11.98	46.09	31.37
F3-90-6 h	279.72	11.76	9.91	45.2	33.13
F3-90-24 h	279.75	11.17	9.07	45.3	34.46
F3-110-6 h	282.14	10.58	8.82	46.14	34.47
F3-110-24 h	283.33	10.37	6.97	46.68	35.89
F4	267.62	13.86	5.42	47.95	31.78
F4-90-6 h	270.06	13.25	3.64	48.13	34.95
F4-90-24 h	271.09	12.64	3.13	49.00	35.30
F4-110-6 h	273.67	12.13	2.20	50.05	35.62
F4-110-24 h	274.00	12.07	2.17	50.10	35.66